Journal of Optoelectronic and Biomedical Materials Vol. 17, No. 4, October-December 2025, p. 303-312

Polymers modified with multilayered metal oxide nanocomposites for targeted drug delivery and ROS-mediated anticancer effects

A. D. Khalid [a], N.-Ur-Rehman [b], G. Shaheen [c], S. Sultana [d], I. Ali [e], M. Zahra [f], M. I. Khan [g], W. Abbasi [a *], Osama A. Mohammed [h], M. Iqbal [i,j]

[a] *University Institute of Radiological Sciences and Medical Imaging Technology, The University of Lahore, Lahore, Pakistan*

[b] *Institute of Physics, The Islamia University of Bahawalpur, Bahawalpur, Pakistan*

[c] *Department of Eastern Medicine, University College of Conventional Medicine, The Islamia University of Bahawalpur, Bahawalpur, Pakistan*

[d] *Department of Eastern Medicine, G.C. University Faisalabad, Pakistan*

[e] *Department of Life Sciences, School of Sciences, University of Management and Technology, Lahore, Pakistan*

[f] *School of Pharmacy and Medical Sciences, Griffith University, Australia*

[g] *Department of Physics, The University of Lahore, Lahore, Pakistan*

[h] *Department of Pharmacology, College of Medicine, University of Bisha, Bisha,61922, Saudi Arabia*

[i] *Renewable Energy and Environmental Technology Centre, University of Tabuk, Tabuk, 47913, Saudi Arabia*

[j] *School of Chemistry, University of the Punjab, Lahore 54590, Pakistan*

Nanocomposites, primarily consisting of metal oxide nanoparticles, have advanced drug delivery and cancer therapy. These nanoparticles are smart for biomedical relevance owing to their biocompatibility, ease of functionalization and capability to generate reactive oxygen species (ROS), which are critical for cancer treatment. This study focuses on the synthesis and characterization of TiO_2 and ZnO NPs along with their nanocomposites, functionalized with polymers of polyethylene glycol (PEG) and folic acid (F.A) individually as well as nanocomposites, and loaded with anti-cancer drug Doxorubicin (DOX). The ROS generation and cytotoxic effects of samples were assessed in human liver cancer cells, demonstrating their potential to induce oxidative stress and cell apoptosis. The results showed that individual nanoparticles produced significant ROS and exhibited higher toxicity, while their composites, particularly modified PEG, F.A and DOX had reduced cytotoxicity. This indicates that the functionalizing NPs can reduce the harmful effects of ROS. Ultimately, these findings highlight the potential of nanoparticle design to enhance therapeutic efficiency while minimizing toxicity to normal tissues, contributing to more effective cancer treatment strategies.

(Received May 30, 2025; Accepted December 24, 2025)

Keywords: Titanium dioxide, Nano composites, Polymers, DOX, HepG2 cells, MTT assay

1. Introduction

In the last few decades, the growth of nanocomposites have revolutionized the field of drug delivery and cancer treatment [1]. The incorporation of metal oxide (MO) nanoparticles (NPs) into polymeric matrices has attracted considerable attention due to their unique properties such as their biocompatibility and potential for functionalization [2]. Among these metal oxide nanoparticles, Titanium dioxide (TiO_2) and Zinc oxide have shown assurance in various medical applications [3].

* Corresponding author: wajida.abbasi@rsmi.uol.edu.pk
https://doi.org/10.15251/JOBM.2025.174.303

The exacting in cancer therapy and functionalized metal oxide with polymers enhances their stability, biocompatibility and drug delivery capability, which offers advantages in controlled drug release, targeted delivery and therapeutic efficiency [4]. The metal oxide NPs have been widely studied for various chemical properties and the capacity to be functionalized with various biomolecules and polymers [5]. These NPs exhibit good dispersion in the biological system and their small size boosts the cellular uptake, particularly in cancer cells [6]. Among these NPs, the TiO_2 and ZnO have been shown to possess anticancer properties by reactive oxygen species (ROS) generation [7]. The use of ROS to medicate anticancer activity has emerged as a potential therapeutic approach; the metal oxide NP can generate ROS under different conditions, including exposure to UV and visible light [8]. These ROS can bring oxidative stress, which disrupts cellular function and leads to cancer cell apoptosis [9]. The polymer functionalization plays a vital role in improving the stability and functionality of metal oxide NPs in drug delivery systems [5].By attaching various functional groups, such as polyethylene glycol (PEG) and polylactic acid (PLA), the physicochemical properties of metal oxide NPs can be tailored [10]. The merging of these polymers can increase the solubility of metal oxide NPs and reduce cytotoxicity. Polymeric coating also allows for conjugation of targeting ligands, such as folic acid (F.A) and peptides, to selectively target specific cancer cells [11, 12].These surface modification enables nanoparticles for drug delivery to the tumor [13]. Many nanostructures have been fabricated due to their distinctive properties in the field of biotechnology [14, 15]. Among these nanostructures, the most used is titanium dioxide (TiO_2) in the biomedical field, such as cosmetics, medicine and pharmaceutical appliances [16, 17]. TiO_2 is available in crystalline forms of Rutile and anatase. The anatase form is more active than rutile in fields of photo-catalytic and cytotoxicity [18].The TiO_2 is also cost effective and less toxic material [19]. TiO_2 also generates ROS under UV radiation [20]. The ROS generation is a new potential for cancer cells' death without affecting the normal cells [21]. ZnO nanoparticles are also known as toxic by generating reactive oxygen species [22]. TiO_2 and its composites with other molecules can be used for cancer therapy [23]. Folic acid (FA) is a polymer that can be used as a good tumor indicator for targeting the cure of cancer cells [24]. Polyethylene Glycol (PEG) is a polyether composite with heaps of medical uses due to its biocompatibility properties [25]. Their biocompatibility can be enhanced for the attachment of PEG to the shell of nanoparticles [26]. Soltani et al., reported that nanoparticles coated with polymers such as PEG enhanced their bioavailability but reduced the toxicity [27]. A. Sani et al., also concluded that nano carriers coated with copolymers (PEG+FA-L) on breast cancer cells and reduced their cytotoxicity [28]. chemotherapy agents such as Camptothecin (CPT), and Doxorubicin (DOX), which are the mainly usually used anticancer drugs [29]. On the other hand, these traditional chemotherapeutic drugs are meanly fractional in use due to their quick aggregation and deficiency under physiological situation, poor allocation in tumors, and cruel side effects to ordinary tissues, which fundamentally reduce their therapeutic efficiency [30] The ROS generated cytotoxic behavior of ZnO, TiO_2 and their composite have already been reported by our earlier article [31].In our study, we initiated the fabrication of TiO_2 nanoparticles, subsequently investigating their reactive oxygen species (ROS) generation upon integration with multi-layers of metal oxides and polymers. This innovative approach sought to evaluate ROS generation via exposure to human liver cancer cells (HepG2), leveraging the destructive potential of oxidative stress to impact cell viability, confirmed through MTT assays [32]. To augment the functionality, TiO_2 was strategically coated with ZnO to engineer composite structures, while the introduction of diverse polymers, such as Folic Acid (F.A.), Polyethylene Glycol (PEG), and the potent cancer drug Doxorubicin (DOX), was orchestrated onto the nanocomposites of (ZnO-TiO_2), thereby fabricating advanced nano-conjugates. Notably, our findings revealed a surprising trend: the effective ROS generation on multi-layered TiO_2 configurations exhibited unexpected decreases, suggesting novel avenues for manipulating ROS production in these composite structures.

2. Materials and methods

The TiO_2, ZnO nanoparticles were synthesized by the sol-gel method and the co-precipitation route, respectively, in the laboratory. The nanocomposites were prepared by the dip coating technique. The nanoparticles, as well as their nanocomposites, were loaded with polymers

of folic acid (FA) and polyethylene glycol (PEG) in a ratio of 1:1. The functionalized samples were loaded with anti-cancer drug Doxorubicin (DOX) by ratio of 1:0.1.

2.1. Synthesis of nanocomposites

The sol-gel and co-precipitation methods were used to synthesize the TiO_2 and ZnO NPs individually. The ZnO-TiO_2 was obtained by depositing ZnO on TiO_2 in two steps, namely, sol-gel and co-precipitation techniques. To synthesize TiO_2 nanoparticles via the sol-gel method, titanium isopropoxide ($C_{12}H_{28}O_4Ti$), nitric acid (HNO_3), distilled water and ethanol were utilized as precursors. 20 ml each of titanium isopropoxide and ethanol were mixed by string following with adding of 24 ml of distilled water. Afterward, 10 ml of 30% HNO_3 was gradually added dropwise to maintain the PH of the solution. The substantial solution was stirred at a constant temperature of 60 °C for four hours until a gel appeared. The gel was then dried at a constant temperature of 80° C in an oven for ten hours. Finally, the TiO_2 NPs were obtained by gridding and annealing the gel for two hours at a temperature of 500 °C.

The co-precipitation method was used to synthesize ZnO NPs. For this plan, a solution of 2.725 g $ZnCl_2$ in 20 ml of distilled water was prepared, then 4.8 g of NaOH in distilled water was added to create a hydroxide solution. The hydroxide solution was added dropwise in $ZnCl_2$ solution at a temperature of 45 °C with continuous stirring. The resultant mixture was stirred for two hours to get white precipitations, which were separated by the process of centrifugation. The ZnO NPs were washed several times with a mixture of distilled water and ethanol, dried in an oven at a temperature of 100 °C for 24 hours, and ground to get ZnO nanoparticles.

The samples carried out functionalization with polymers of polyethylene glycol (PEG) and folic acid (FA) in a 1:1 volume ratio to get nano conjugates of F.A-PEG-TiO_2 and F.A-PEG-ZnO. The functionalized process implicated a dip-coating method, where prepared ZnO and TiO_2 NPs were dipped into PEG solution, sonicated at room temperature for two hours, washed with ethanol and dried in an oven at 80 °C. Afterward, a folic acid polymer solution was prepared by process of stirring 25 g of folic acid into 25 ml of Dimethyl sulfoxide (DMSO) and the samples were in this solution. After sonication, washing with distilled water, and drying at a temperature of 60 °C, the samples F.A-PEG-TiO_2 and F.A-PEG-ZnO-TiO_2 NPs were attained.

The anti-cancer drug, Doxorubicin (DOX) was loaded on the outer surface of functionalized nanocomposites. A dispersion of NPs in ethanol (5 mg/mL) was mixed with DOX solution in ethanol (0.5 mg/mL) at a volume ratio of 1: 0.1 to get the DOX-F.A-PEG-ZnO-TiO_2 sample. The ready samples were incubated at a temperature of 25 °C for 60 minutes, then centrifuged at 8000 rpm for 15 minutes. The resulting NPs pellet was suspended in distilled water, collected, freeze-dried, and used for further analysis.

2.2. Characterization of nanoparticles and composites

The Scanning electron microscope (SEM) imaging was used to study the shapes and morphology of TiO_2, ZnO, and ZnO-TiO_2 NPs, providing direct particle size information. The crystalline size and phase of the prepared samples (TiO_2, ZnO, and ZnO-TiO_2) nanoparticles were analyzed using X-ray diffraction (XRD) patterns. The Frontier™ FT-IR spectrometer reflected the FT-IR band in (%) absorbance mode within the range of 600 cm^{-1} to 3500 cm^{-1} for samples of ZnO NPs, ZnO-TiO_2, F.A-PEG-TiO_2, F.A-PEG-ZnO-TiO_2, and DOX-F.A-PEG-ZnO-TiO_2 nano-conjugates.

2.3. Cell culturing and in vitro anticancer activity

The human liver cancer cells (HepG2) were obtained from the Cell and Tissue Culture Bank at the Institute of Molecular Biology and Biotechnology (IMBBB). They were cultured in T75 and T25 flasks under standard environment at a temperature of 37 °C, followed 95% relative humidity, and a 5% CO_2 atmosphere. The effectiveness of cellular growth and intracellular delivery of samples and cells was evaluated using a phase-contrast compound microscope. Cell washing was carried out in triplicate using phosphate-buffered saline (PBS) at 7.4 PH. Cell pellets were obtained through centrifugation, and the cells were suspended in Dulbecco's Modified Eagle Medium (DMEM) including fetal bovine serum (FBS) at a concentration of 10% (v/v). Cell counting was performed using a hemocytometer. For treatment, cancer cells are seeded into well plates at a density of 6.0 ×

10^5 cells per well and incubated for twenty-four hours. Subsequently, dispersions of all nanoparticles and their composites were added to the cells to assess their anticancer potential.

To evaluate the proliferative potential of the cell lines, a 3-(4,5-dimethylthiazol-2-yl)-5-diphenyltetrazolium bromide (MTT) assay was conducted [33]. Cells cultured on 96-well plates were used for this assay. Initially, the cell monolayer was washed with PBS (Invitrogen Inc., USA) and then incubated with 100 µl of medium containing 25 µl of MTT solution (Invitrogen Inc., USA) for two hours at 37 °C. MTT changes color to purple formazan in viable cells, which was solubilized using 10% sodium dodecyl sulfate (SDS), and the absorbance of the solution was calculated at 570 nm by a spectrophotometer.

ROS generation by the prepared nanoparticles was assessed in human liver cancer cells (HepG2). Cells were seeded in a 6-well plate at a density of 3.0×10^5 cells and incubated for twenty-four hours at 37°C. TiO_2, ZnO NPs, their composites, and those functionalized with polymers F.A and PEG, as well as DOX, were applied to induce cell death, incubating the samples with the cells for twenty-four hours. Following incubation, the samples were removed, and the cells were washed at least three times. The population percentage of the control group (no treatment) was considered as 100%, and the treated group was compared based on ROS generation. Every experiment was carried out in triplicate, and the data were calculated as the mean with standard deviation.

3. Results and discussion

The crystal phase and crystalline size of the fabricated sample TiO_2, ZnO NPs and their nanocomposites ZnO-TiO_2 were investigated by the XRD technique. Figure 1 describes the XRD patterns of TiO_2, ZnO and their nanocomposites. The range of 2 theta, 20^0–60^0 was used to draw the XRD patterns. Figure 1 revealed diffraction peaks at 25^0 and 48^0, which showed the crystalline nature of TiO_2 and ZnO NPs, which depicts that the anatase phase of TiO_2 and the hexagonal wurtzite structure of ZnO NPs. Their structure remains the same in their composites. JCPDS File No. 900-9086, 900-8123 and 500-0223 confirm their structure.

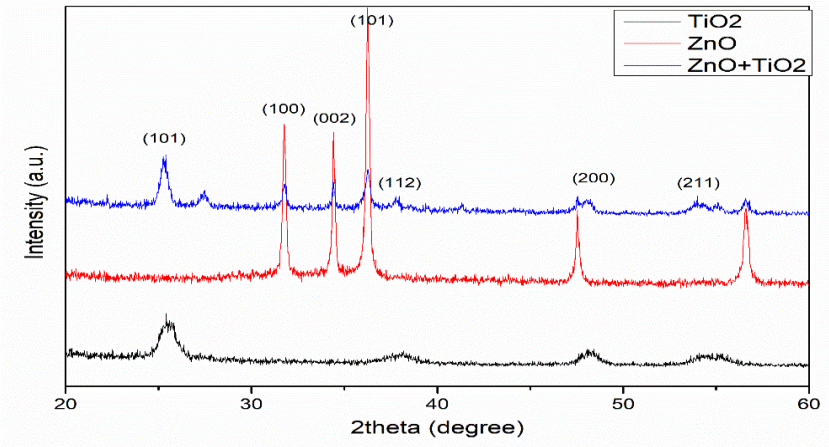

Fig. 1. XRD pattern of TiO_2, ZnO and their composites ZnO-TiO_2.

Scherer's formula was used to measure the crystalline size. The Scherer's formula [34] is given by

$$D = \frac{k\lambda}{\beta cos\theta}$$

The full width at half maximum (FWHM) of peaks, denoted by β, relates to the X-ray diffraction study. The wavelengths of X-rays (λ) and the diffraction angle (θ) are integral parameters in determining crystallite sizes. Upon analysis, the average crystallite sizes were measured as 15.03 nm for TiO_2, 37.93 nm for ZnO, and within the range of 37.99-14.45 nm for their composites.

SEM imaging was in use to examine the morphology of these nanoparticles. The resulting SEM images, presented in Fig. 2, depict the fabricated nanoparticles. In the first image portraying TiO_2, the particles exhibit a small circular form with an average diameter of 10 nm, maintaining a uniform morphology throughout. Contrastingly, the second image illustrating ZnO particles shows a rod-shaped structure with a non-uniform columnar growth pattern, averaging 40 nm in diameter. The morphology of the ZnO nanoparticles reveals a nanostructure with numerous broken and agglomerated features. The third image presents the nano-composites, displaying various particles dispersed onto non-uniform, larger agglomerated particles. Additionally, this image highlights the presence of both nano-rods and smaller particles distributed separately, indicating that the individual shapes of TiO_2 and ZnO particles remain unchanged within their composites

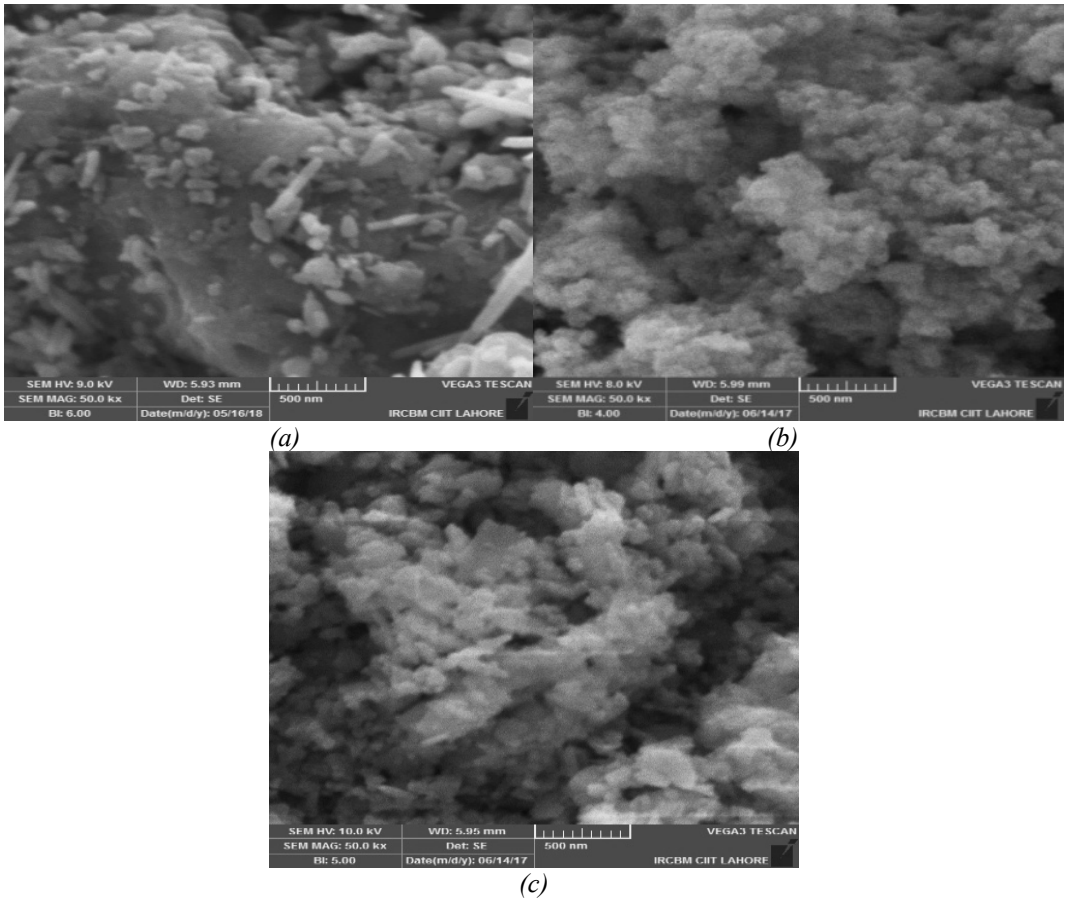

Fig. 2. (a) SEM image of TiO2 NPs; (b) SEM image of ZnO NPs; (c) SEM image ZnO-TiO_2nano-composite.

Figure 3 shows the graphs of FTIR spectra aimed at TiO_2, ZnO NPs and nanocomposites. Figure 3(a) indicates the TiO_2, where the peak 1630 cm^{-1} shows the squally mode of the water Ti-OH [35]. Figure 3(b) denotes ZnO, where in the graph, peaks 687 and 743 cm^{-1} represents ZnO conferring to the literature assessment, the peaks between 450-800 $cm^{-1}$are spreading vibrations of Zn-O [36]. Figure 3(c) signifies their composite(ZnO-TiO_2). The peak 1383 cm^{-1} represents Ti-O [37, 38]. The peak at 3440 $cm^{-1,}$ which is in the range 3400-3450 cm^{-1}, describes the O-H extending vibration, which represents water. Peak of 1420 cm^{-1} is due to equal extension of zinc [39]. Band at 1025 cm^{-1} is due to C-O extending vibration [40].Figure 3(d) is FTIR spectra of functionalized

composite ($ZnO\text{-}TiO_2$) with polymers polyethylene glycol (PEG) and folic acid (F.A). Various peaks show the existence of PEG, the peak at 1100 cm^{-1} is owing to C-H meandering and C-O extending vibration, while the peak at 1242 cm^{-1} represents C-H blowy vibrations [41, 42]. These peaks express the presence of PEG. The presence of F.A in the composite is described by peak 1519 cm^{-1}(Phenyl and pterin ring),1604 cm^{-1}(NH bending), approved with the literature conforms the existence of folic acid [43]. The wrapper of $ZnO\text{-}TiO_2$-PEG-F.A with Doxorubicin (DOX), is described by Figure 3(e) which describes the connections between ZnO and DOX, many peaks of graph at 1615 cm^{-1} (CO–H), 1283 cm^{-1} (O–H···O, C–H, and C–OH), and 988 cm^{-1} (C–C=O, C–OH, and aliphatic C–H) cm^{-1} are the spectrum of DOX [44]. Figure 3(f) represents the TiO_2 functionalized with PEG and F.A. The peaks in the peaks at graph clarify the existence of F.A and PEG. The peaks 1100, 1242, and 1604 cm^{-1} are described in Figure 3 (d).The peaks 3322 cm^{-1} at 1511 cm^{-1}describethe presence of folic acid as the peak range 1485-1519 $cm^{-1}$and 3100-3500 $cm^{-1}$for folic acid [43]. The Ti-O stretching is at peak 1383 cm^{-1} as described in Figure 3(c).

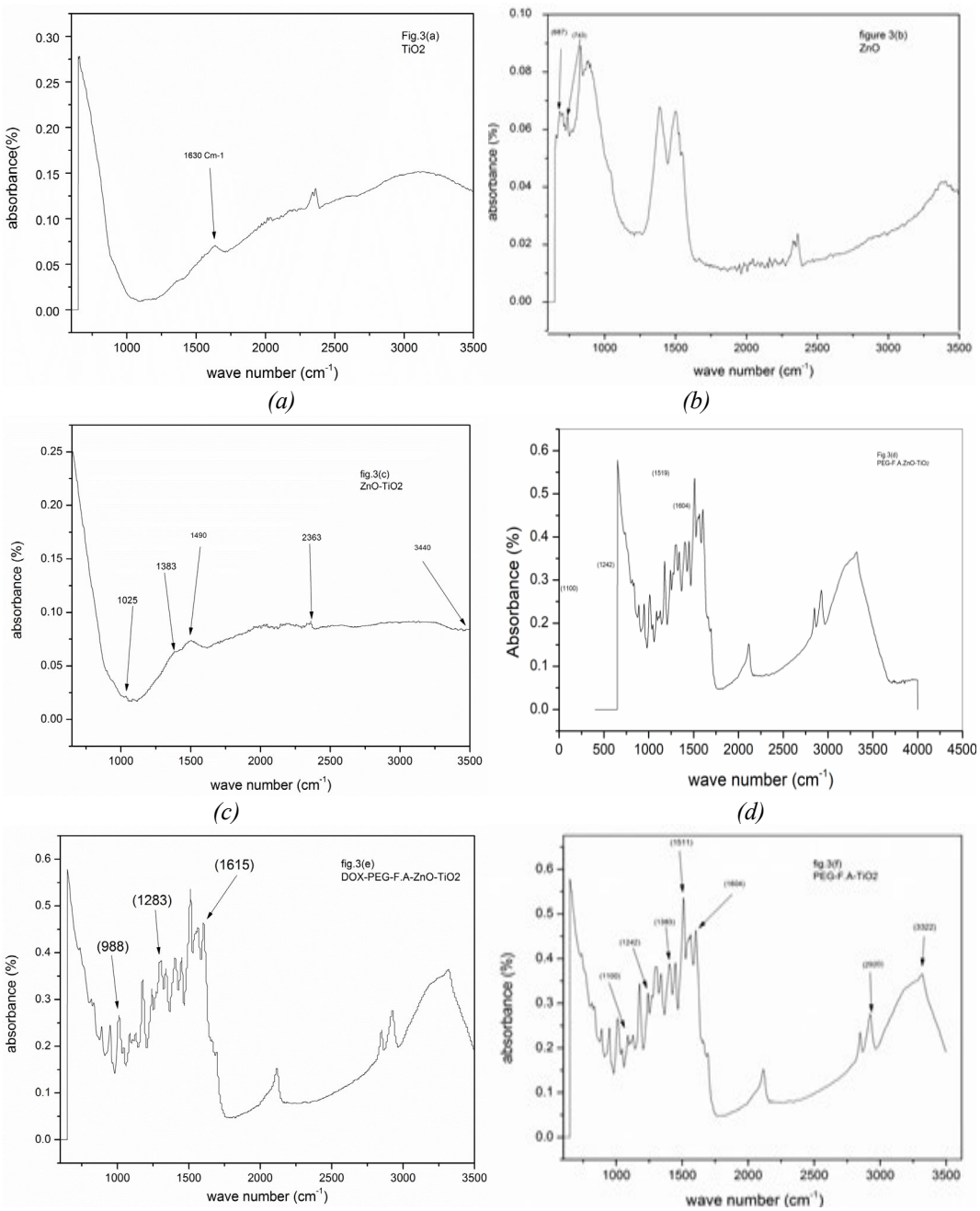

Fig. 3. (a) FTIR spectra of TiO_2; (b) FTIR spectra of ZnO; (c) FTIR spectra of $ZnO\text{-}TiO_2$; (d) FTIR spectra of PEG-F.A-$ZnO\text{-}TiO_2$; (e) FTIR spectra of DOX-PEG-F.A-$ZnO\text{-}TiO_2$; (f) FTIR spectra of PEG-F.A-TiO_2.

HepG2 cells were utilized for in vitro assessment of the anti-cancer potential of various samples by examining their ability to induce Reactive Oxygen Species (ROS) generation. Cell viability was evaluated using a colorimetric MTT assay that measures the absorbance of light at a wavelength of 570 nm, directly correlating with the number of living cells [45, 46]. Metal oxide nanoparticles (NPs) demonstrated cytotoxic effects on cancer cells through the induction of cellular oxidative stress, showcasing biocompatibility with liver function [47]. Cytotoxicity of each sample (i.e., TiO_2, ZnO, their composites, polymers coated and DOX loaded) proved their cytotoxicity, however cell viability of individual TiO_2 and ZnO was less than other samples either their composites, functionalized by polymers or loaded with DOX, as shown in graph, the intracellular ROS up-regulation can produce oxidative stress which might carry to apoptosis [48]. Previously, it proven that metal oxide NPs can bring apoptosis in human cancer cells by generating reactive oxygen species [49]. The cell viability of the cells treated by individual TiO_2 and ZnO was significantly less than that of the polymers coated, DOX and composites of TiO_2 and ZnO groups. It proves that ROS generated by individual TiO_2 and ZnO nanoparticles is more than their composites, functionalized with PEG, F.A and DOX. The individual NPs revealed a greater ROS generation as compared to the other groups, which is due to their larger cellular access and cytotoxicity knockdown mechanism. The same reduction of cytotoxicity was also reported in core-shell structure, i.e., when one type of NPs was covered with a second one [50, 51]. Parallel properties of toxicity decrease have been gotten when SiO_2 and ZrO_2 were used as compound materials with TiO_2 [52]. In addition, it is reported that single TiO_2 NPs might strengthen in vivo anticancer behavior via the generation of ROS in tumor tissues. The anticancer activity of $TiO_2$is reduced when made into composites with ZnO, or coated with polymers, which is anticipated to reduce ROS generation.

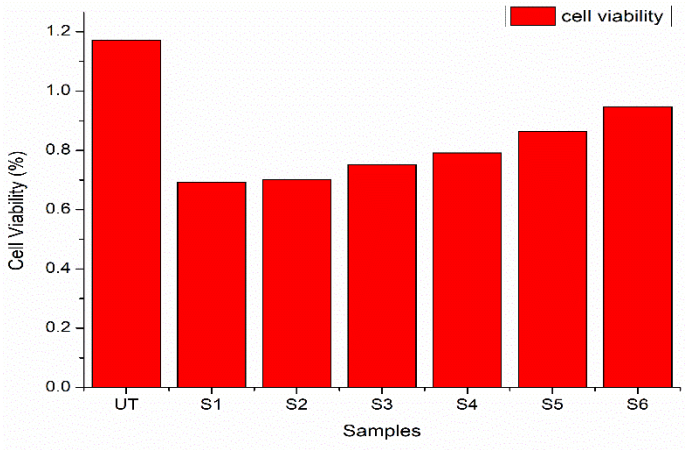

Fig. 4. Cell viability; UT= untreated cells S1=TiO_2, S2=ZnO, S3=PEG-F.A-TiO_2, S4=ZnO-TiO_2, S5=PEG-F.A-ZnO-TiO_2, S6=DOX-PEG-F.A-TiO_2.

4. Conclusion

This study demonstrates the promising potential of metal oxide nanoparticles, particularly in cancer therapy and investigates their ability, in combination with multi-layered metal oxides and polymers, to generate Reactive Oxygen Species affecting human liver cancer cells viability. Synthesis of TiO_2 and ZnO nanoparticles, along with their ZnO-TiO_2 composites, was successful using sol-gel and co-precipitation methods, resulting in distinct crystalline structures confirmed by XRD analysis. Scherer's formula determined their crystalline sizes, consistent with XRD patterns, while SEM imaging illustrated TiO_2 as uniform circular particles and ZnO as rod-like structures with irregular growth. FTIR spectra validated characteristic peaks for TiO_2, ZnO, their composites, and modified forms with PEG, F.A., and DOX, affirming successful functional group attachments.

In vitro HepG2 cell assessments revealed varied cytotoxicity among samples, notably higher in individual TiO_2 and ZnO nanoparticles than in their composites or modified counterparts, indicating significant ROS generation from individual nanoparticles, potentially due to their access and cytotoxic mechanisms. Importantly, ROS production and cytotoxicity were reduced in composite, polymer-coated, or DOX-loaded nanoparticles, suggesting a strategy to mitigate their cytotoxic impact via modifications. This study illuminates the intricate relationship between nanoparticle structure, modifications, ROS generation, and their influence on cancer cell viability, offering pathways for tailored nanoparticle designs in targeted anticancer therapies. Thus, further optimization of these nanoparticle-based systems could lead to more efficient and less toxic cancer therapies in the future.

Acknowledgements

The authors are thankful to the Deanship of Graduate Studies and Scientific Research at University of Bisha for supporting this work through the Fast-Track Research Support Program.

References

[1] Gupta, A., et al., Future Journal of Pharmaceutical Sciences, 2025. 11(1): p. 37; https://doi.org/10.1186/s43094-025-00789-4

[2] Zadehnazari, A., Polymer-Plastics Technology and Materials, 2023. 62(5): p. 655-700; https://doi.org/10.1080/25740881.2022.2129387

[3] Muhammad, N.A.M., N.A. Awang, H. Basri, Optik, 2023. 283: p. 170855. https://doi.org/10.1016/j.ijleo.2023.170855

[4] Yassin, M.T., et al., Cancers, 2024. 16(24): p. 4234; https://doi.org/10.3390/cancers16244234

[5] Vasić, K., Ž. Knez, and M. Leitgeb, Journal of Functional Biomaterials, 2024. 15(8): p. 227; https://doi.org/10.3390/jfb15080227

[6] Georgeous, J., et al., Pharmaceutics, 2024. 16(10): p. 1332; https://doi.org/10.3390/pharmaceutics16101332

[7] Karthikeyan, C., et al., International Journal of Biological Macromolecules, 2023. 242: p. 124814; https://doi.org/10.1016/j.ijbiomac.2023.124814

[8] Canaparo, R., et al., Materials, 2020. 14(1): p. 53; https://doi.org/10.3390/ma14010053

[9] Hayes, J.D., A.T. Dinkova-Kostova, K.D. Tew, Cancer cell, 2020. 38(2): p. 167-197; https://doi.org/10.1016/j.ccell.2020.06.001

[10] Ramezani Dana, H. F. Ebrahimi, Polymer Engineering & Science, 2023. 63(1): p. 22-43; https://doi.org/10.1002/pen.26193

[11] Sarkar, S., et al., Journal of Nanoparticle Research, 2012. 14: p. 1-24; https://doi.org/10.1007/s11051-011-0715-2

[12] Choudhury, H., et al., Current Pharmaceutical Design, 2020. 26(42): p. 5365-5379; https://doi.org/10.2174/1381612826666200721000958

[13] Ahmed, A., et al., Expert opinion on drug delivery, 2021. 18(1): p. 1-24; https://doi.org/10.1080/17425247.2020.1822321

[14] Goswami, R.K., et al., Biocatalysis and Agricultural Biotechnology, 2024: p. 103330; https://doi.org/10.1016/j.bcab.2024.103330

[15] Tyagi, R., A. Maurya, Titanium Dioxide-Based Multifunctional Hybrid Nanomaterials: A Comprehensive Study of Their Biological Applications, in Titanium Dioxide-Based Multifunctional Hybrid Nanomaterials: Application on Health, Energy and Environment. 2025, Springer. p. 291-312; https://doi.org/10.1007/978-3-031-80625-4_13

[16] Poon, T.K.C., K.P. Iyengar, V.K. Jain, Journal of Clinical Orthopaedics and Trauma, 2021. 21: p. 101536; https://doi.org/10.1016/j.jcot.2021.101536

[17] Jafari, S., et al., International Journal of Nanomedicine, 2020. 15: p. 3447; https://doi.org/10.2147/IJN.S249441

[18] Sharma, R., J. Prakash, TiO2 Nanomaterials: Synthesis, Properties, Modifications, and Applications, in Titanium Dioxide-Based Multifunctional Hybrid Nanomaterials: Application on Health, Energy and Environment. 2025, Springer. p. 1-25; https://doi.org/10.1007/978-3-031-80625-4_1

[19] Gatou, M.-A., et al., Reactions, 2024. 5(1): p. 135-194; https://doi.org/10.3390/reactions5010007

[20] Nagaraj, K., et al., Next Research, 2025: p. 100180; https://doi.org/10.1016/j.nexres.2025.100180

[21] Sahoo, B.M., et al., Anti-Cancer Agents in Medicinal Chemistry-Anti-Cancer Agents), 2022. 22(2): p. 215-222; https://doi.org/10.2174/1871520621666210608095512

[22] Ravi, P., et al., Journal of Cluster Science, 2025. 36(1): p. 1-36; https://doi.org/10.1007/s10876-024-02733-7

[23] Ziental, D., et al., Nanomaterials, 2020. 10(2): p. 387; https://doi.org/10.3390/nano10020387

[24] Dayekh, F.R., et al., Applied Organometallic Chemistry, 2025. 39(4): p. e70110; https://doi.org/10.1002/aoc.70110

[25] Gosecki, M., et al., Polymers, 2016. 8(6): p. 227; https://doi.org/10.3390/polym8060227

[26] Hatamie, S., et al., Polymers for Advanced Technologies, 2025. 36(2): p. e70094; https://doi.org/10.1002/pat.70094

[27] Soltani, M., et al., Toxicology in Vitro, 2025. 105: p. 106022; https://doi.org/10.1016/j.tiv.2025.106022

[28] Sani, A., et al., Journal of Drug Delivery Science and Technology, 2023. 86: p. 104642; https://doi.org/10.1016/j.jddst.2023.104642

[29] Jia, T., et al., Molecular pharmaceutics, 2017. 14(8): p. 2529-2537; https://doi.org/10.1021/acs.molpharmaceut.6b00708

[30] Anand, U., et al., s. Genes & diseases, 2023. 10(4): p. 1367-1401; https://doi.org/10.1016/j.gendis.2022.02.007

[31] Khalid, A.D., et al., Chemosphere, 2023. 310: p. 136885; https://doi.org/10.1016/j.chemosphere.2022.136885

[32] Pei, J., et al., Molecules, 2024. 29(11): p. 2706; https://doi.org/10.3390/molecules29112706

[33] Pattabhi, A., M. Arun, M. Krishnan, Cuestiones de Fisioterapia, 2025. 54(3): p. 2908-2916.

[34] Khan, Z., et al., Chalcogenide Letters, 2024. 21(11); https://doi.org/10.15251/CL.2024.2111.933

[35] León, A., et al., Applied Sciences, 2017. 7(1): p. 49; https://doi.org/10.3390/app7010049

[36] Dayakar, T., et al., Materials Science and Engineering: C, 2017. 75: p. 1472-1479; https://doi.org/10.1016/j.msec.2017.02.032

[37] Abazović, N.D., et al., The Journal of Physical Chemistry B, 2006. 110(50): p. 25366-25370; https://doi.org/10.1021/jp064454f

[38] Mugundan, S., et al., Applied Nanoscience, 2015. 5(4): p. 449-456; https://doi.org/10.1007/s13204-014-0337-y

[39] Chithra, M.J., M. Sathya, K. Pushpanathan, EActa Metallurgica Sinica (English Letters), 2015. 28(3): p. 394-404; https://doi.org/10.1007/s40195-015-0218-8

[40] Sharma, R., et al., Journal of Materials Chemistry C, 2014. 2(38): p. 8142-8151; https://doi.org/10.1039/C4TC01056F

[41] Venkatasubbu, G.D., et al., Advanced Powder Technology, 2013. 24(6): p. 947-954; https://doi.org/10.1016/j.apt.2013.01.008

[42] Naghibi, S., et al., Ceramics International, 2014. 40(4): p. 5481-5488; https://doi.org/10.1016/j.ceramint.2013.10.136

[43] He, Y., et al., Spectrochimica acta part A: molecular and biomolecular spectroscopy, 2009. 72(4): p. 876-879; https://doi.org/10.1016/j.saa.2008.12.021

[44] Das, G., et al., FT-IR, Microscopy research and technique, 2010. 73(10): p. 991-995; https://doi.org/10.1002/jemt.20849

[45] Kim, S., S.Y. Lee, H.-J. Cho, Nanomaterials, 2017. 7(11): p. 354; https://doi.org/10.3390/nano7110354

[46] Bhilkar, P., et al., Materials Research, 2024. 169: p. 81-112; https://doi.org/10.21741/9781644903261-4

[47] Wang, Y.-L., et al., Environmental Pollution, 2024: p. 123617; https://doi.org/10.1016/j.envpol.2024.123617

[48] Sun, Y.-J., L. Liu, and L. Cheng, Chemical Communications, 2020. 56(48): p. 6484-6487; https://doi.org/10.1039/D0CC02245D

[49] Yu, Y., et al., MedComm, 2024. 5(4): p. e519; https://doi.org/10.1002/mco2.519

[50] Hsiao, I.-L. and Y.-J. Huang, Chemical research in toxicology, 2011. 24(3): p. 303-313; https://doi.org/10.1021/tx1001892

[51] Lu, X., et al., Chemical Society Reviews, 2024; https://doi.org/10.1039/D3CS01026K

[52] El-Bassyouni, G.T., et al., Central-European journal of immunology, 2017. 42(1): p. 54; https://doi.org/10.5114/ceji.2017.67318